A structural change on ligand binding underpins the ability of human fatty acid binding protein-1 to potentiate the activity of peroxisome proliferator-activated receptor α agonists

Supporting information

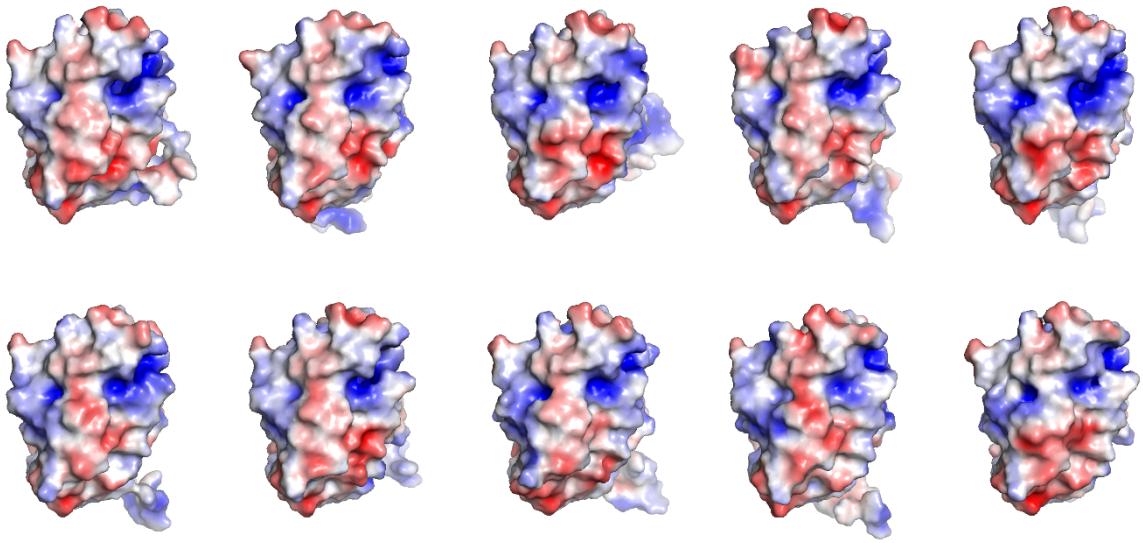

Supplementary Figure 1. Electrostatic surface potential of 10 NMR conformers for *apo* FABP1 (PDB ID 6DO6). Colour coding is as follows: -3kT (red) 3kT (blue).

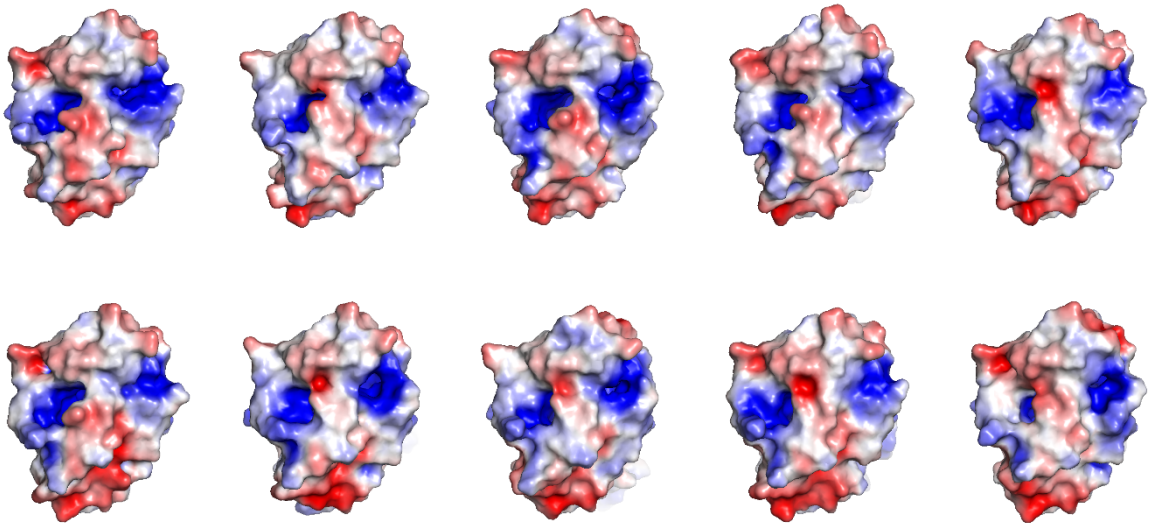

Supplementary Figure 2. Electrostatic surface potential of 10 NMR conformers for GW7647-FABP1 complex (PDB ID 6DO7) reflecting the change in surface exposure of charged residues in the portal loops. Colour coding is as follows: -3kT (red) 3kT (blue).

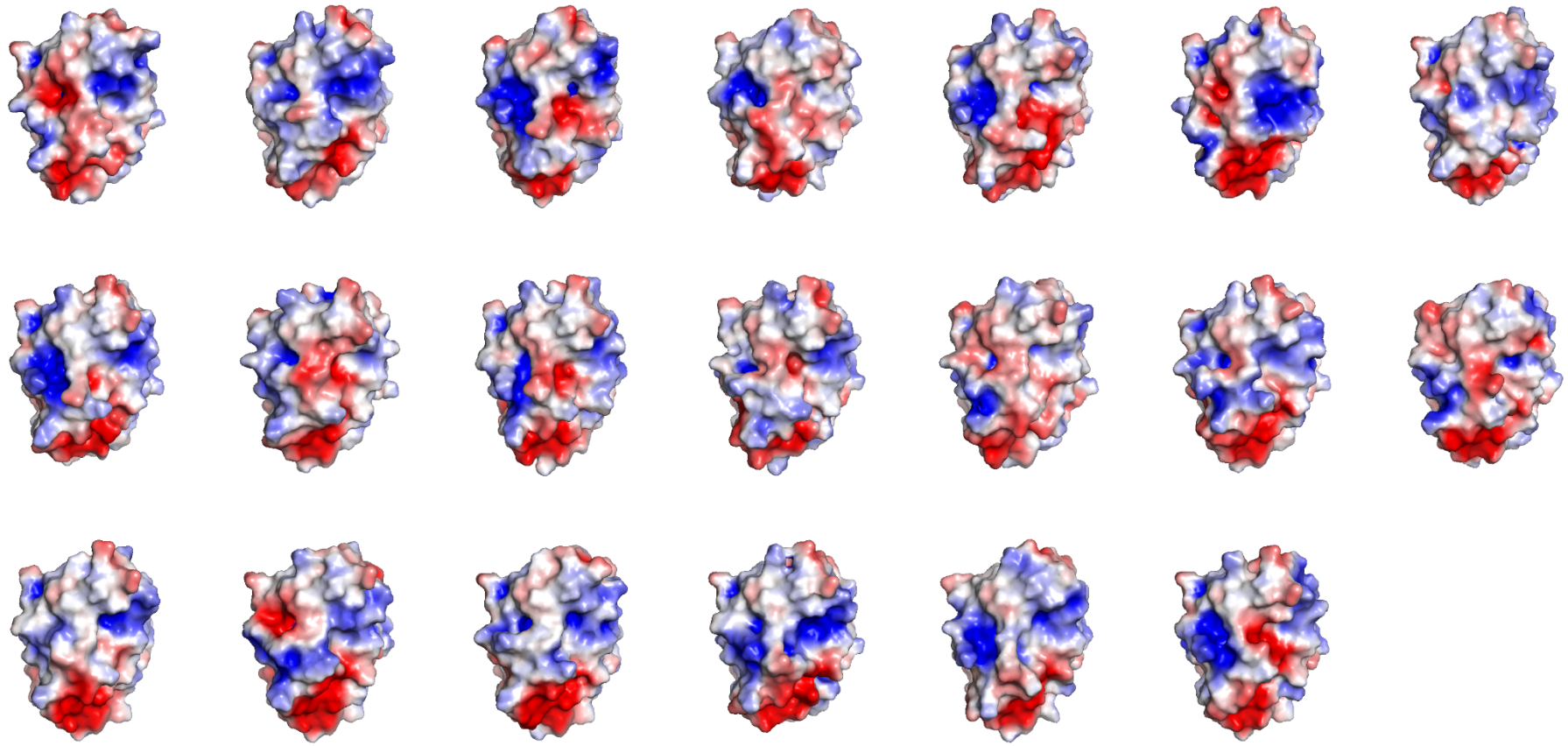

Supplementary Figure 3. Electrostatic surface potential of 20 NMR conformers for *apo* FABP1 (PDB ID 2L67). Colour coding is as follows: -3kT (red) 3kT (blue).

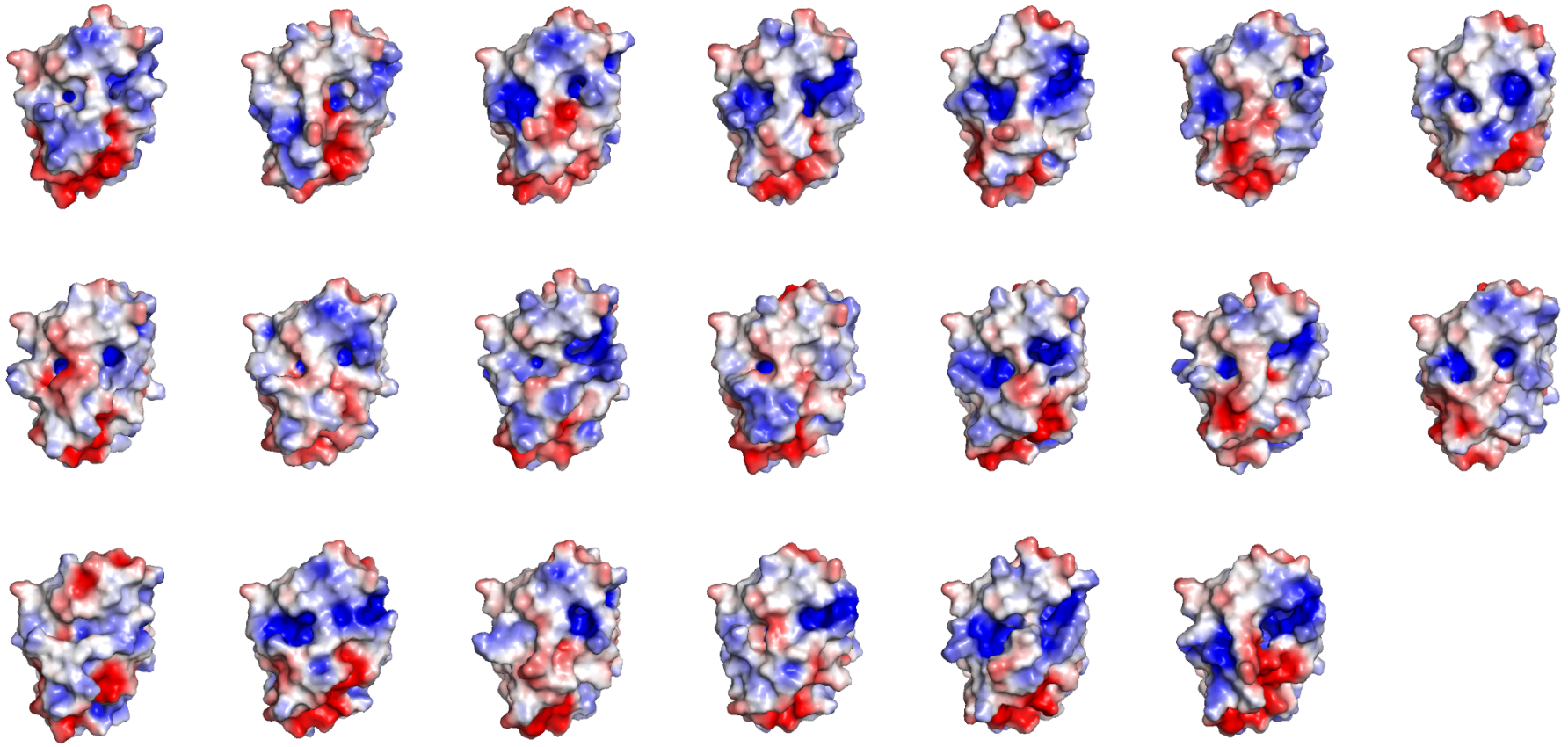

Supplementary Figure 4. Electrostatic surface potential of 20 NMR conformers for Oleate-FABP1 complex (PDB ID 2L68). Colour coding is as follows: -3kT (red) 3kT (blue).

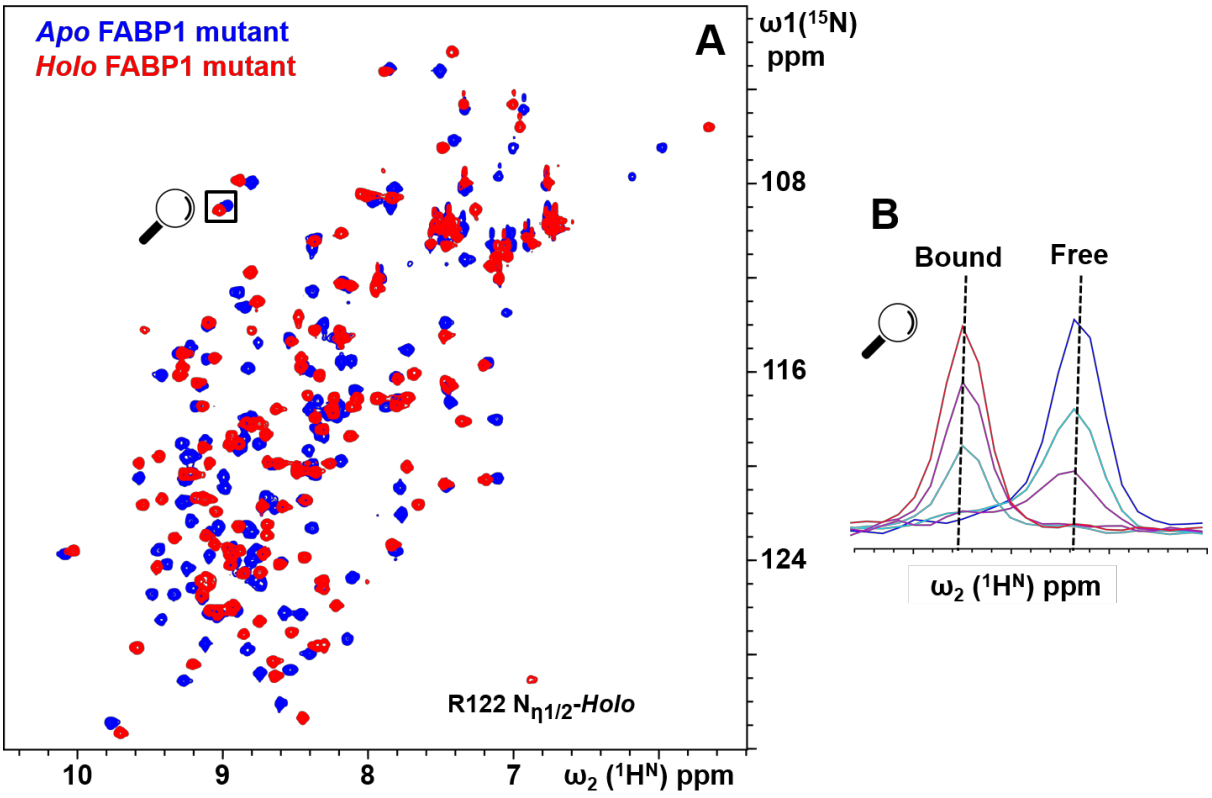

Supplementary Figure 5. Analysis of GW7647 binding to the triple mutant Lys57Ala, Glu77Ala, Lys95Ala FABP1. **(A)** 2D ^{15}N-HSQC of mutant FABP1 in the absence (blue) and presence (red) of a saturating concentration of GW7647. The aliased peak for the guanidinium proton of Arg122 that appears in the spectrum upon addition of GW7647 is labelled. **(B)** Cross section of the highlighted peak upon titration of FABP1 with GW7647. The data indicate that the complex is in slow exchange on the NMR timescale where cross peaks are observed in the titration whose intensity reflects the proportion of *apo* and *holo* mutant FABP1.

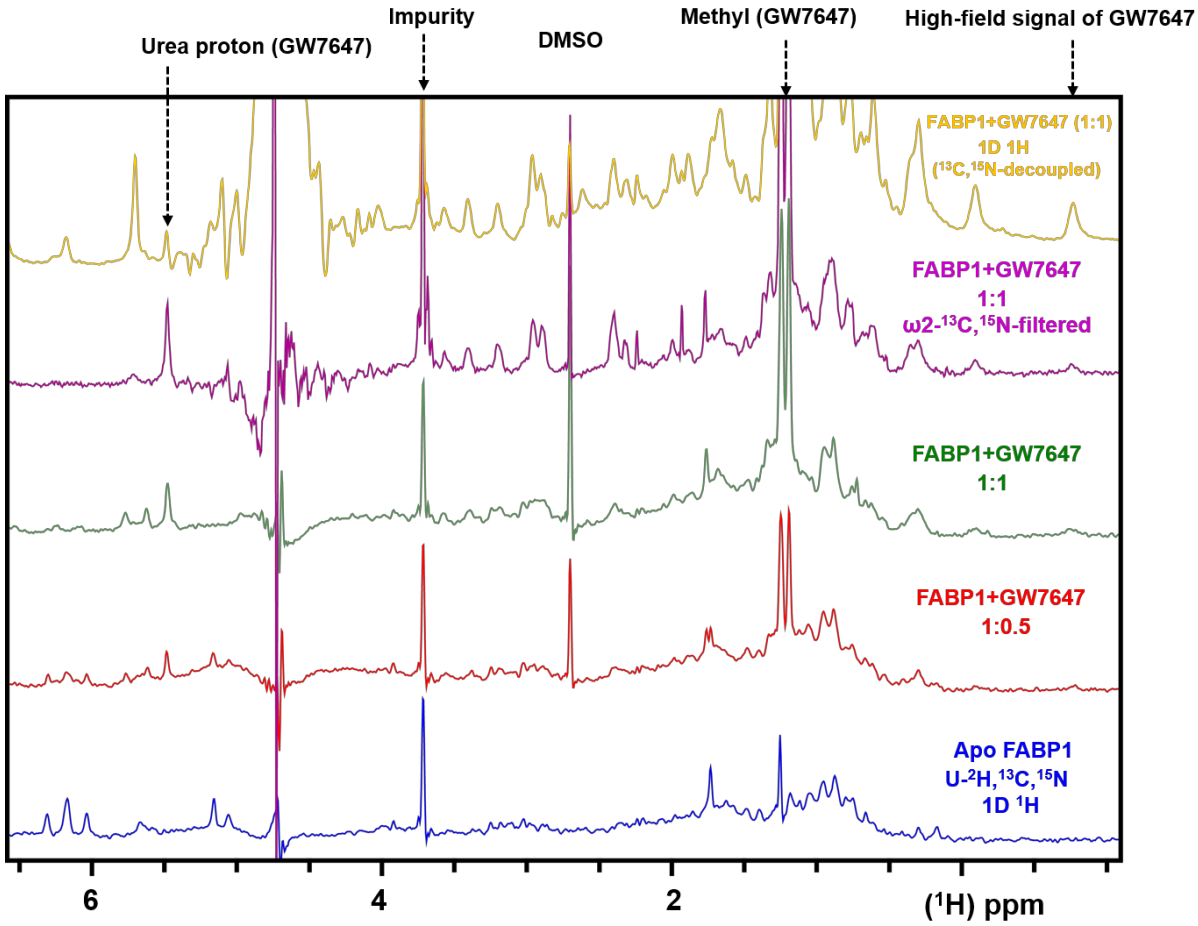

Supplementary Figure 6. Observation of GW7647 resonances in 1D ^{1}H NMR spectra of the complex with FABP1. Stacked spectra show 1D ^{1}H spectra for wt FABP1 in the absence (blue) and in the presence of GW7647 at a molar ratio FABP1:GW7647 of 1:0.5 (red) and 1:1 (green). Also shown are the first FID of 2D ω1-edited, ω2-filtered [^{1}H,^{1}H]-NOESY acquired with WATERGATE solvent suppression (magenta). and a 1D ^{1}H spectrum acquired using a PRESAT pulse sequence with ^{13}C and ^{15}N-decoulping (yellow). The high field aliphatic resonances and the low-field urea signal from GW7647 are labelled.

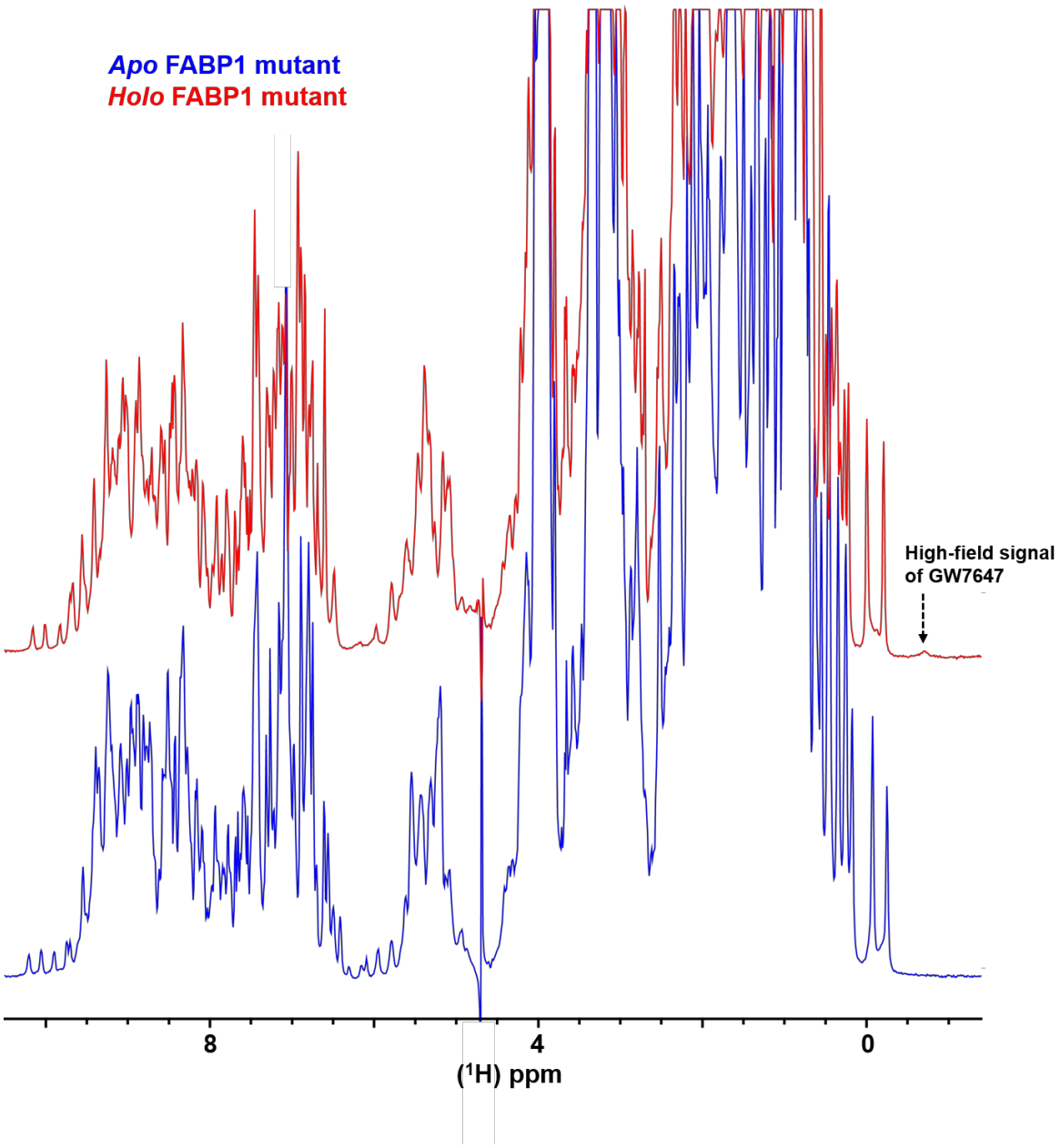

Supplementary Figure 7: Overlay of 1D ^{1}H NMR spectra of mutant FABP1 in the absence (blue) and presence (red) of a saturating concentration of GW7647. The high-filed signal of GW7647 that is also observed in the complex with wt FABP1 is indicated.

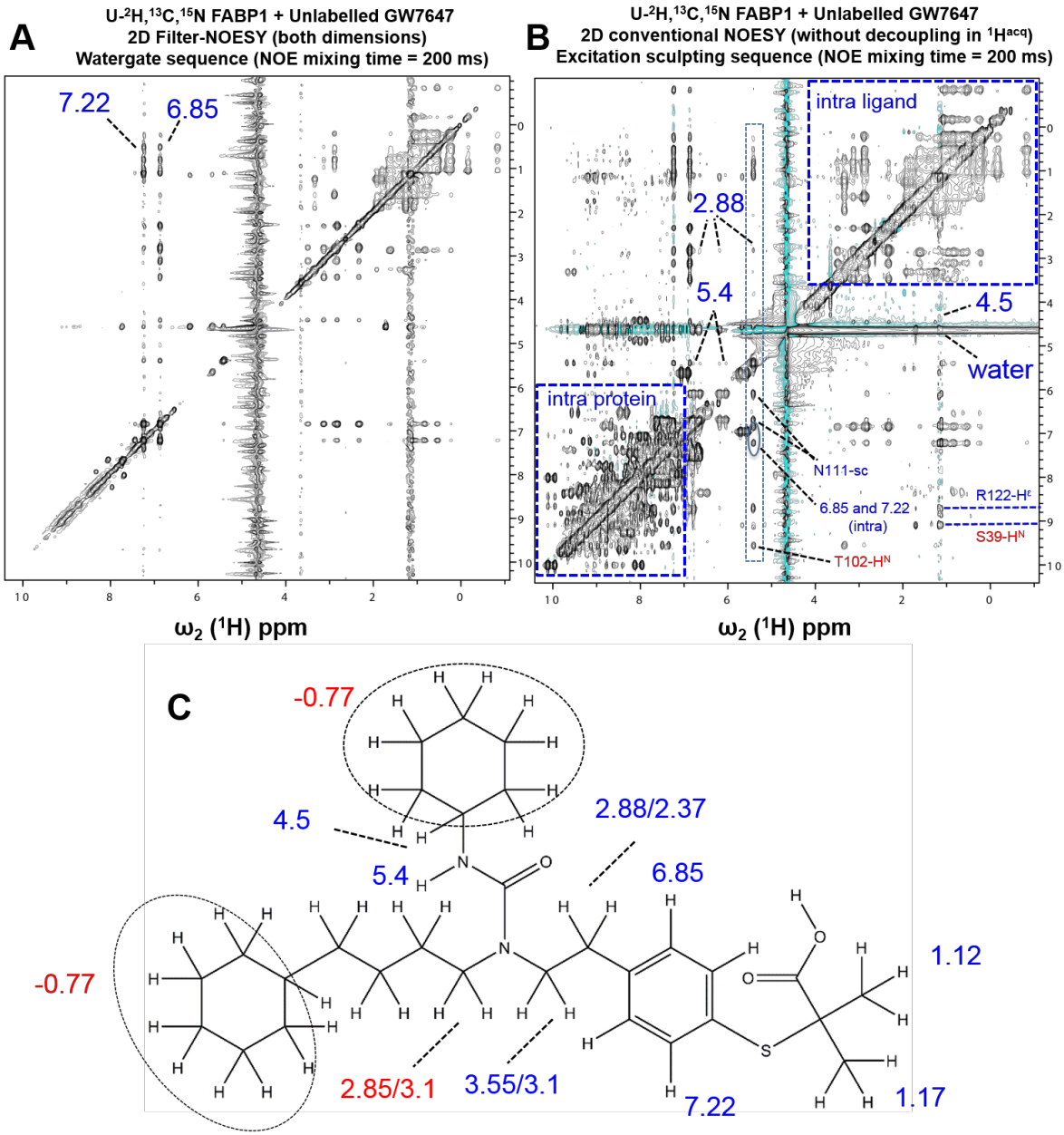

Supplementary Figure 8. 2D [^{1}H,^{1}H]-NOESY spectra of GW7647 in complex with wt FABP1. **(A)** 2D ω1-filtered, ω2-filtered [^{1}H,^{1}H]-NOESY and **(B)** conventional 2D [^{1}H,^{1}H]-NOESY spectra from [U-^{2}H, ^{13}C,^{15}N]-labelled FABP1 (1 mM) and unlabelled GW7647 (1 mM). Some of the intermolecular NOE cross peaks are indicated on the 2D NOESY spectra. Cross peaks with unambiguous assignments are labelled in blue. Some of the peaks for which no unambiguous assignments could be made are labelled in red. Ambiguity arises due to the chemical shift degeneracy of protons in the aliphatic portion of GW7647. **(C)** Structure of GW7647. Unambiguous proton assignments in the complex state are indicated on the structure in blue. Some of the unassigned resonances which are observed in the spectra are shown in red.

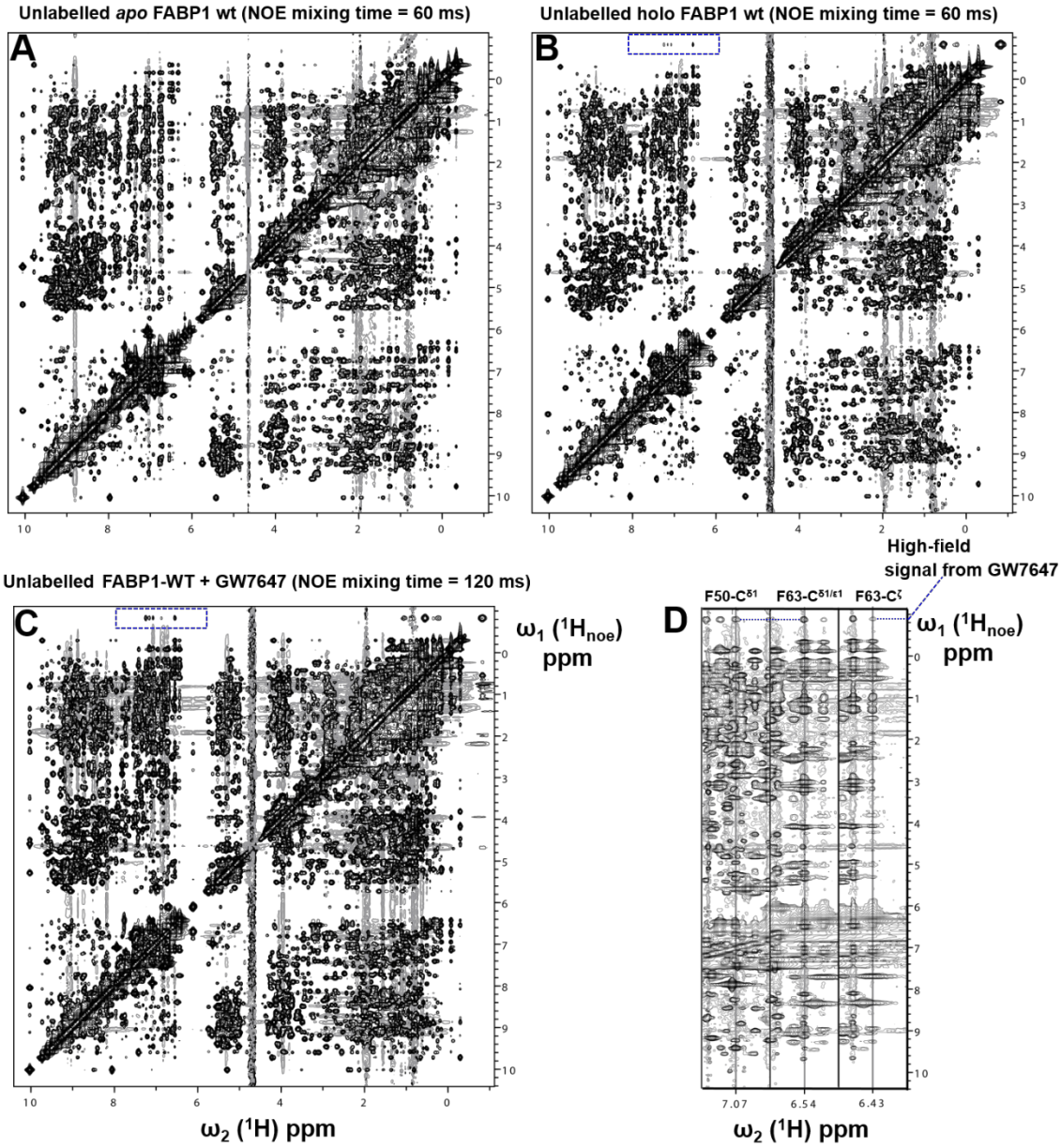

Supplementary Figure 9. 2D [^{1}H,^{1}H]-NOESY spectra of unlabelled FABP1 (1.8 mM) in the absence and presence of unlabelled GW7647 (1.8 mM) at 35 °C. (A) *apo* FABP1 wt with NOE mixing time of 60 ms. (B) *holo* wt FABP1 with NOE mixing time of 60 ms and (C) *holo* wt FABP1 with NOE mixing time of 120 ms. Intermolecular NOE cross peaks between FABP1 and GW7647 are highlighted in blue boxes. (D) Zoomed region of (C) showing intermolecular NOE cross peaks between the high field resonance of GW7647 and aromatic side chains of FABP1 are highlighted. These intermolecular NOEs were not used as distance constraints in the structure calculations as it was not possible to unambiguously assign the resonance at 0.77 ppm to any specific aliphatic proton of GW7647.

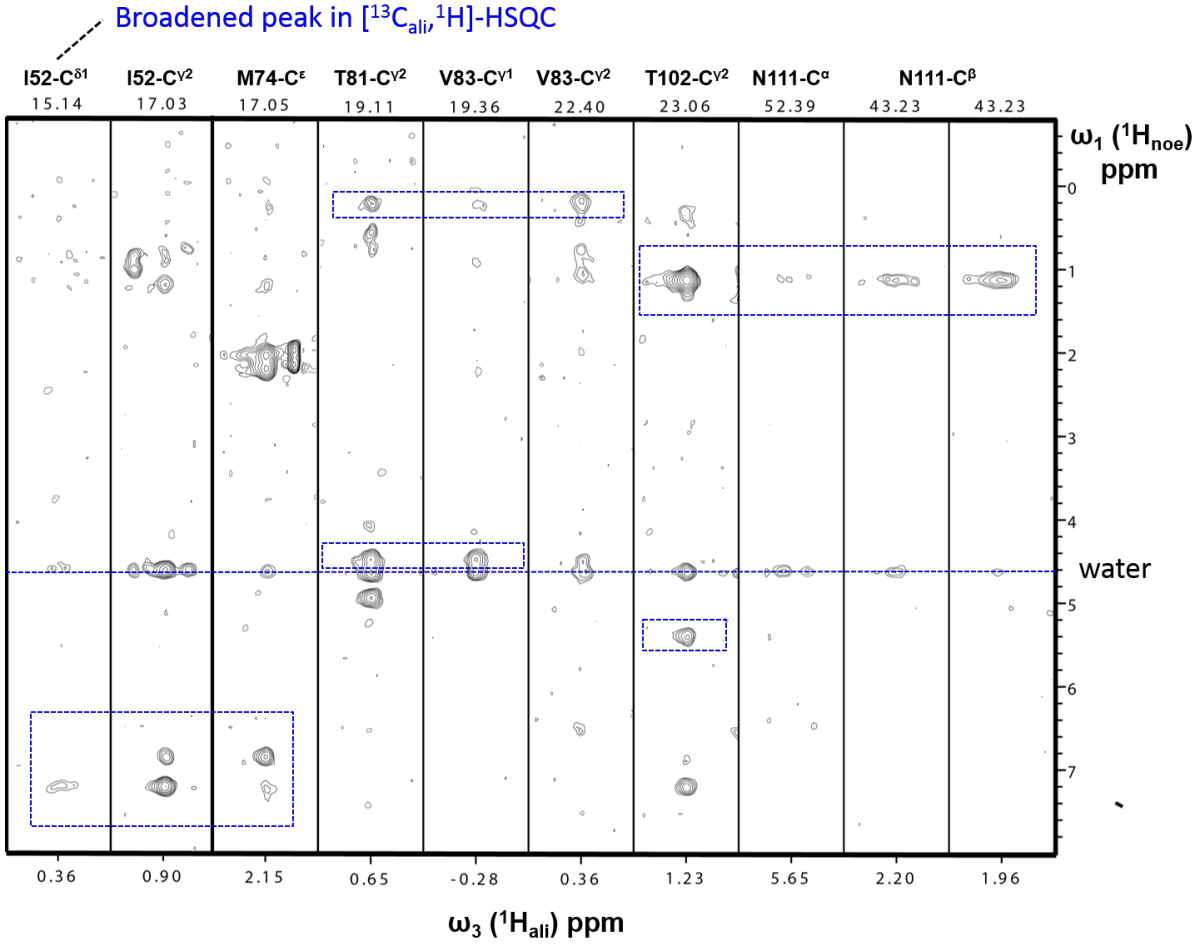

Supplementary Figure 10. 2D [^{1}H,^{1}H]-NOESY strips from the 3D ω1-filtered, ω3(methyl) edited-NOESY spectrum. 3D ω1-filtered, ω3-edited-NOESY data was acquired at 800 MHz and 35 °C from a [U-^{13}C,^{15}N]-labelled FABP1 (0.5 mM) and unlabelled GW7647 (0.5 mM). Intermolecular NOEs observed in the data are highlighted in blue boxes.

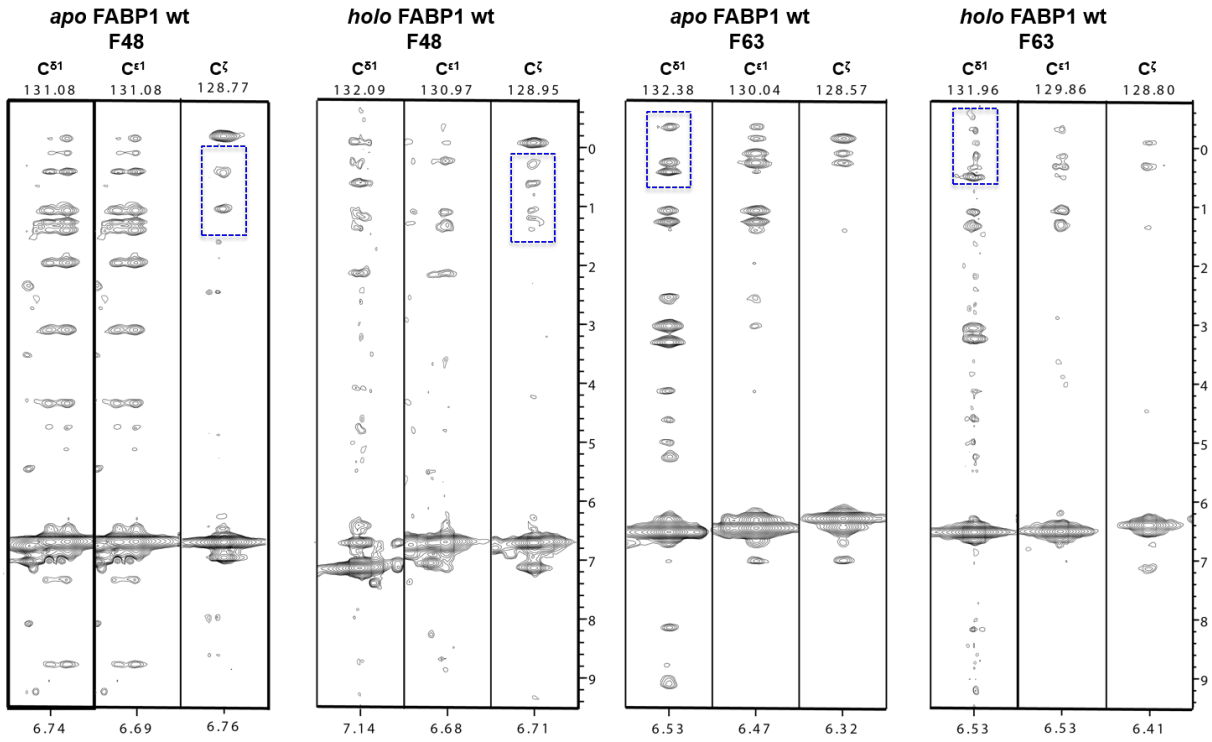

Supplementary Figure 11A. 2D [^{1}H,^{1}H] strips from 3D $^{13}C_{aro}$ resolved-[^{1}H,^{1}H]-NOESY spectrum of FABP1 in the absence (*apo*) and presence (*holo*) of GW7647. Regions showing different patterns of NOE cross peaks in the presence and absence of GW7647 are highlighted in blue boxes.

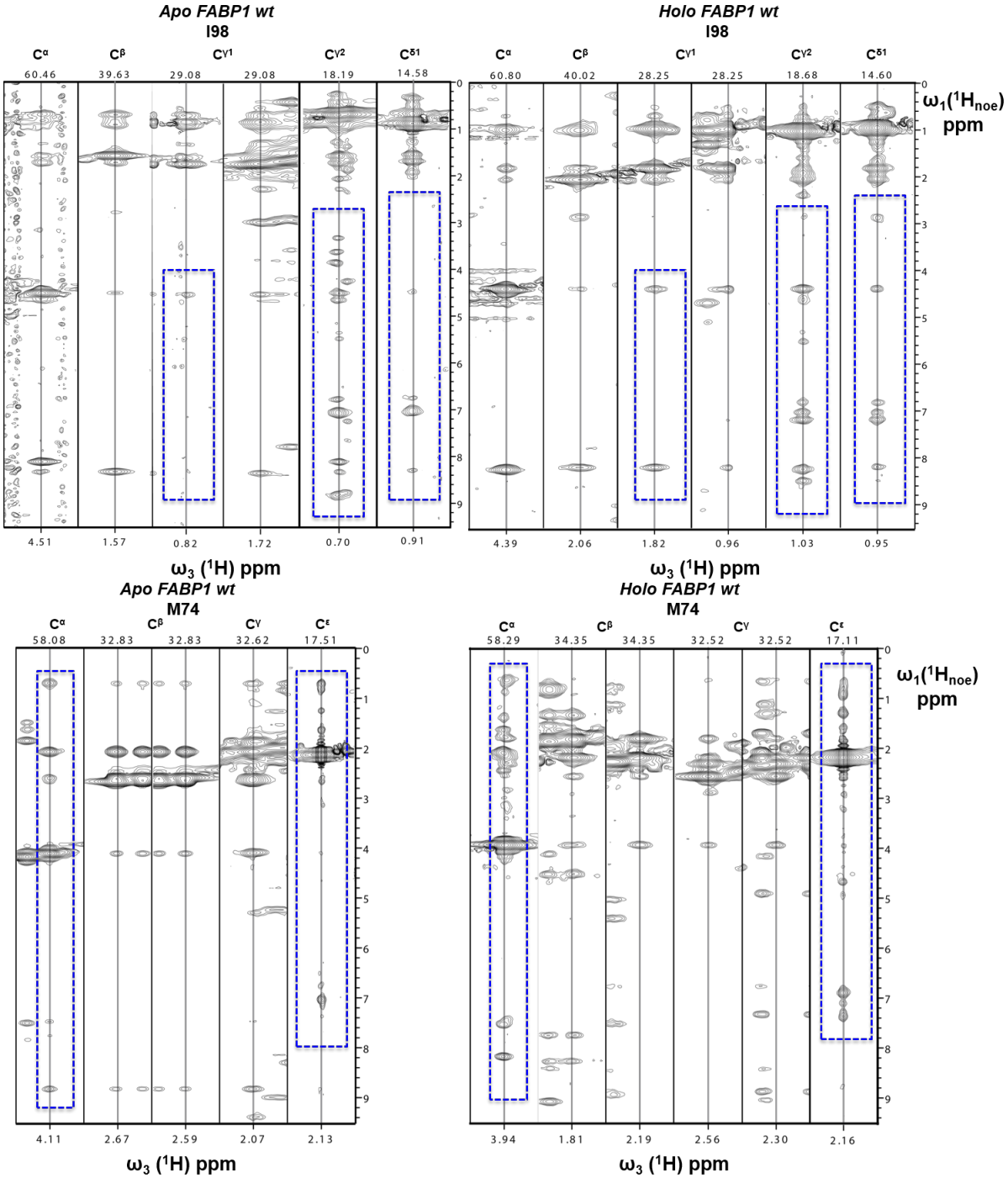

Supplementary Figure 11B. 2D [^{1}H,^{1}H] strips from 3D $^{13}C_{ali}$ resolved-[^{1}H,^{1}H]-NOESY spectrum of FABP1 in the absence (*apo*) and presence (*holo*) of GW7647. Regions showing different patterns of NOE cross peaks in the presence and absence of GW7647 are highlighted in blue boxes.

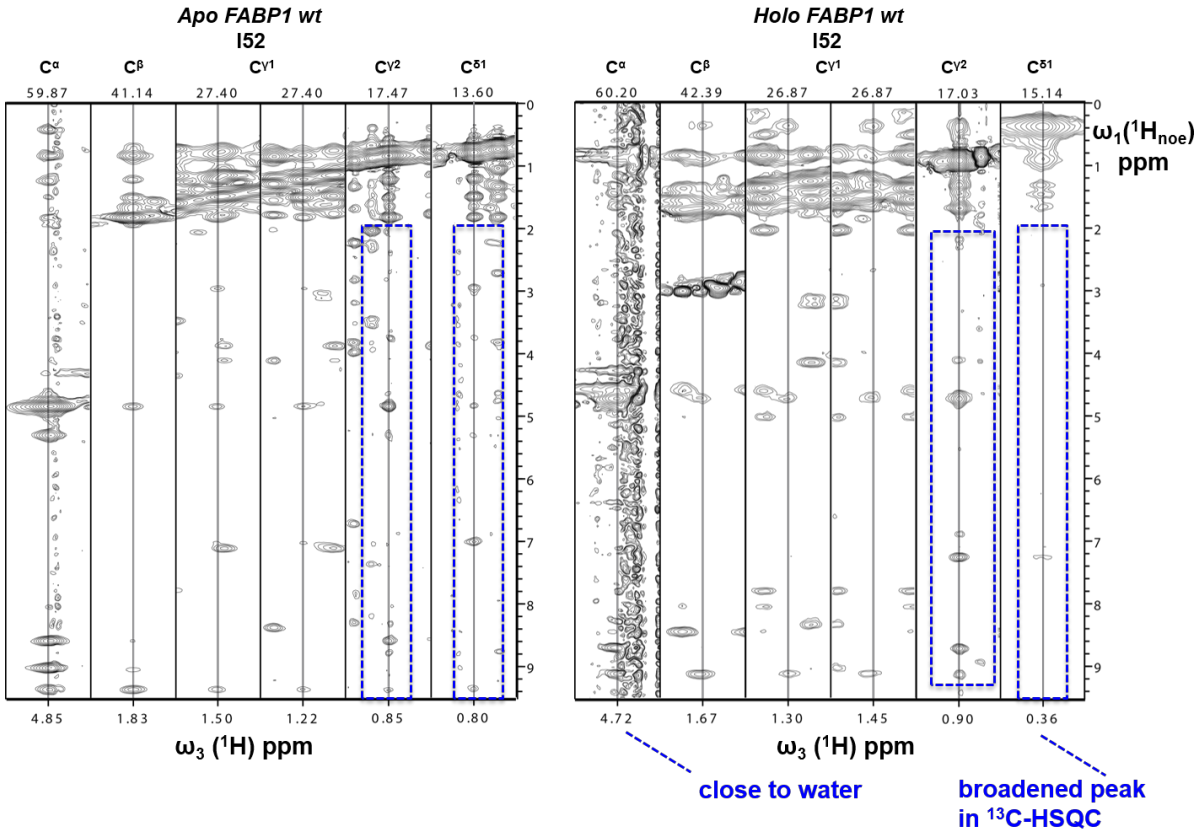

Supplementary Figure 11C. 2D [^{1}H,^{1}H] strips from 3D $^{13}C_{ali}$ resolved-[^{1}H,^{1}H]-NOESY spectrum of FABP1 in the absence (*apo*) and presence (*holo*) of GW7647. Regions showing different patterns of NOE cross peaks in the presence and absence of GW7647 are highlighted in blue boxes.

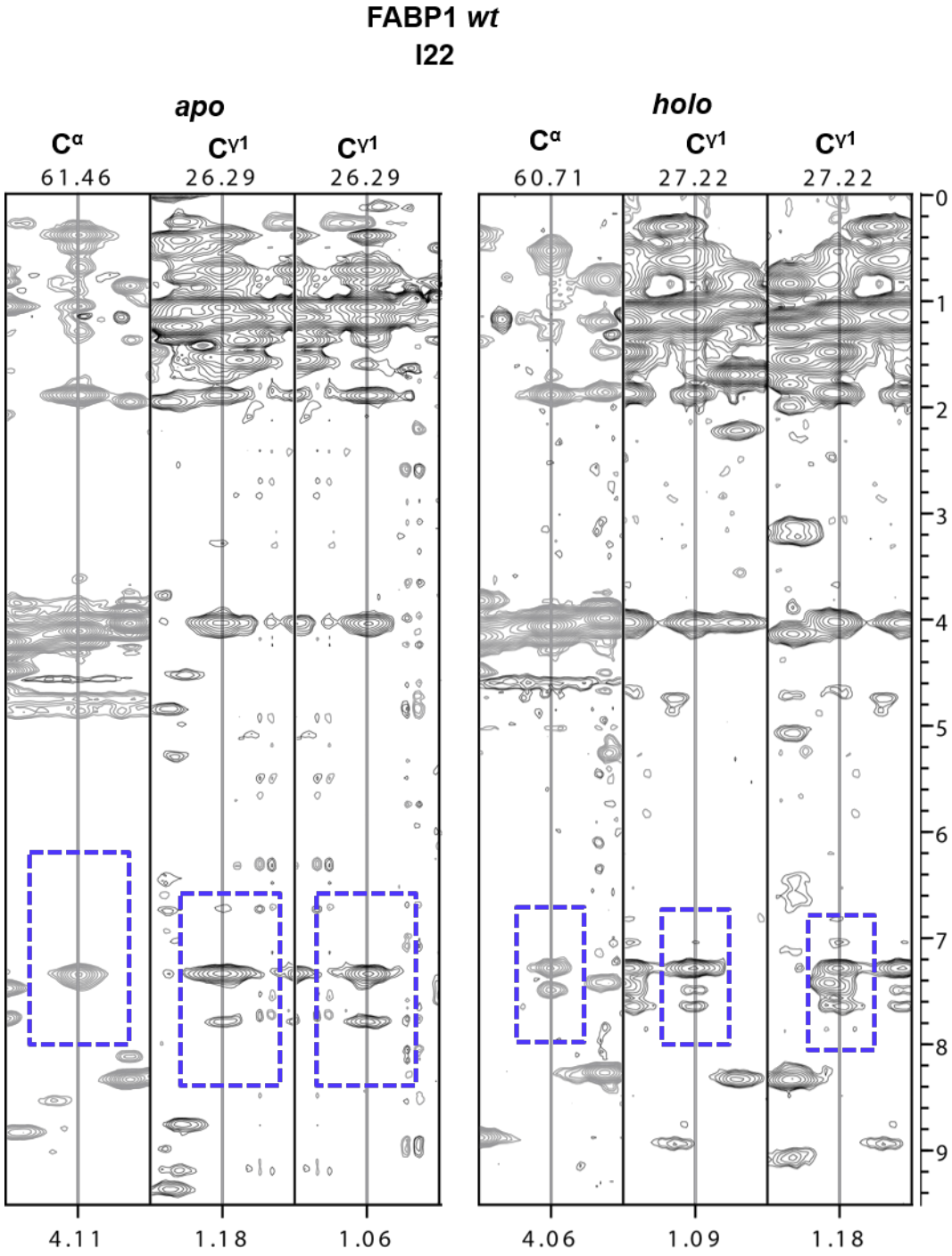

Supplementary Figure 11D. 2D [^{1}H,^{1}H] strips from 3D $^{13}C_{ali}$ resolved-[^{1}H,^{1}H]-NOESY spectrum of FABP1 in the absence (*apo*) and presence (*holo*) of GW7647. Regions showing different patterns of NOE cross peaks in the presence and absence of GW7647 are highlighted in blue boxes.

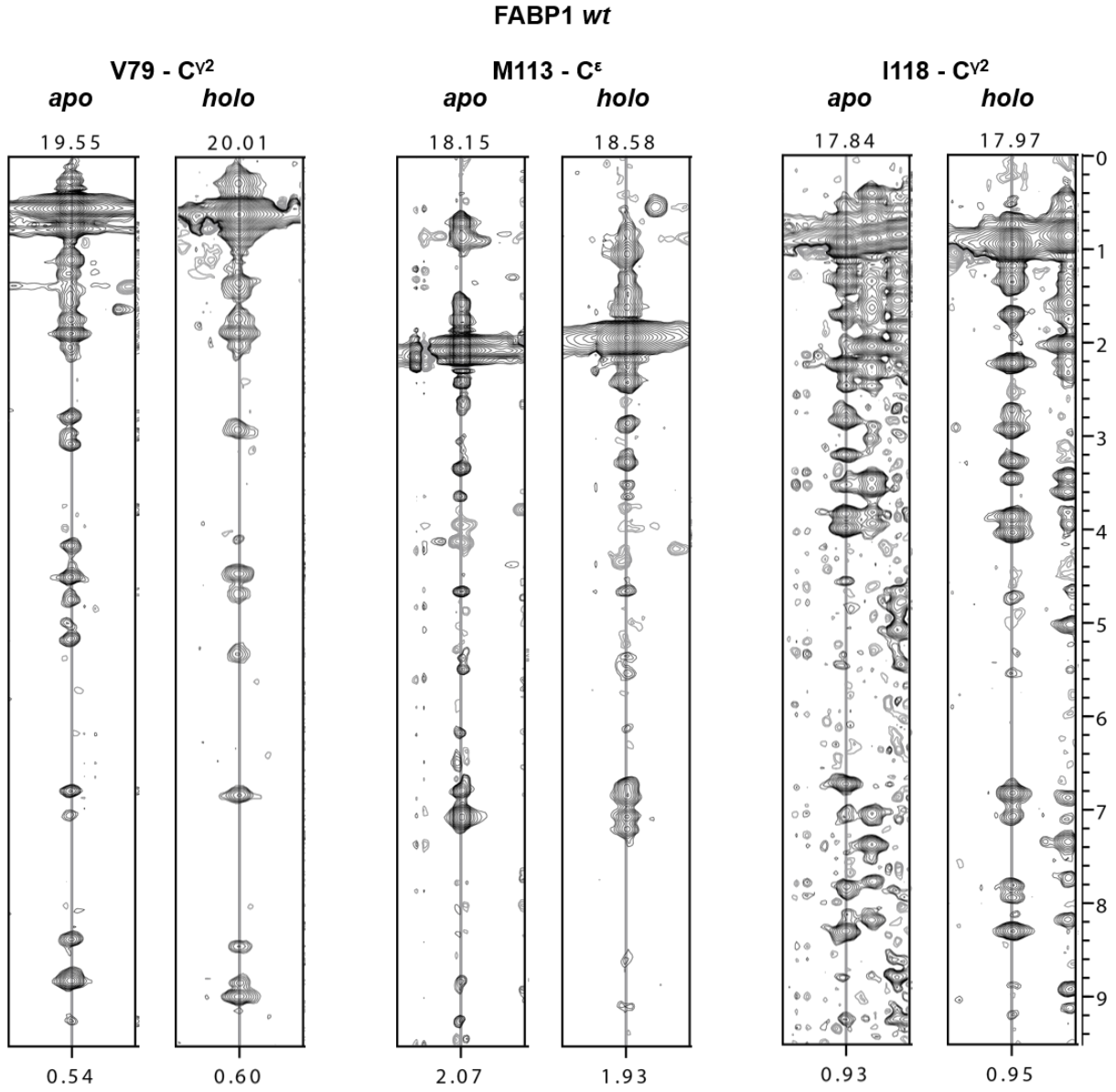

Supplementary Figure 11E. 2D [^{1}H,^{1}H] strips from 3D $^{13}C_{ali}$ resolved-[^{1}H,^{1}H]-NOESY spectrum of FABP1 in the absence (*apo*) and presence (*holo*) of GW7647.

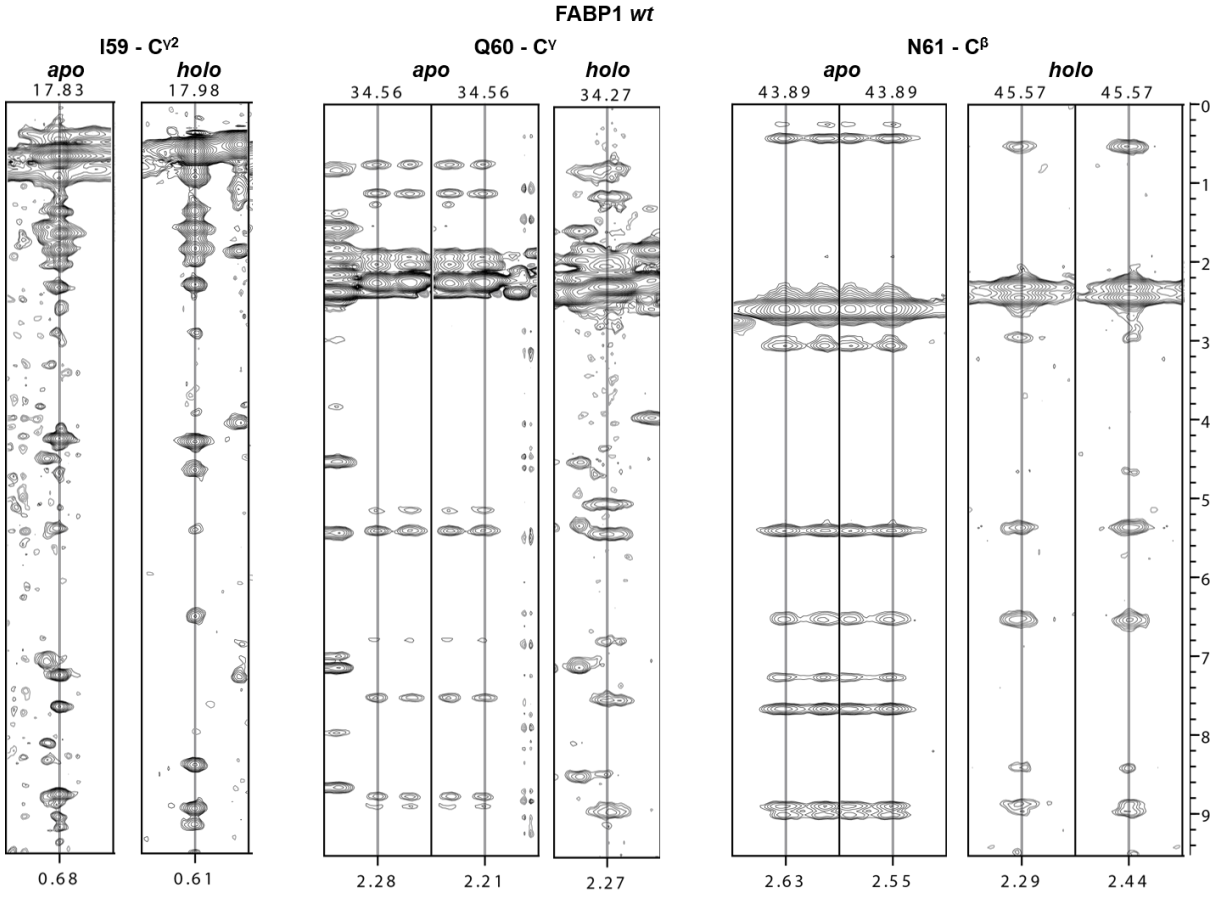

Supplementary Figure 11F. 2D [^{1}H,^{1}H] strips from 3D $^{13}C_{ali}$ resolved-[^{1}H,^{1}H]-NOESY spectrum of FABP1 in the absence (*apo*) and presence (*holo*) of GW7647.

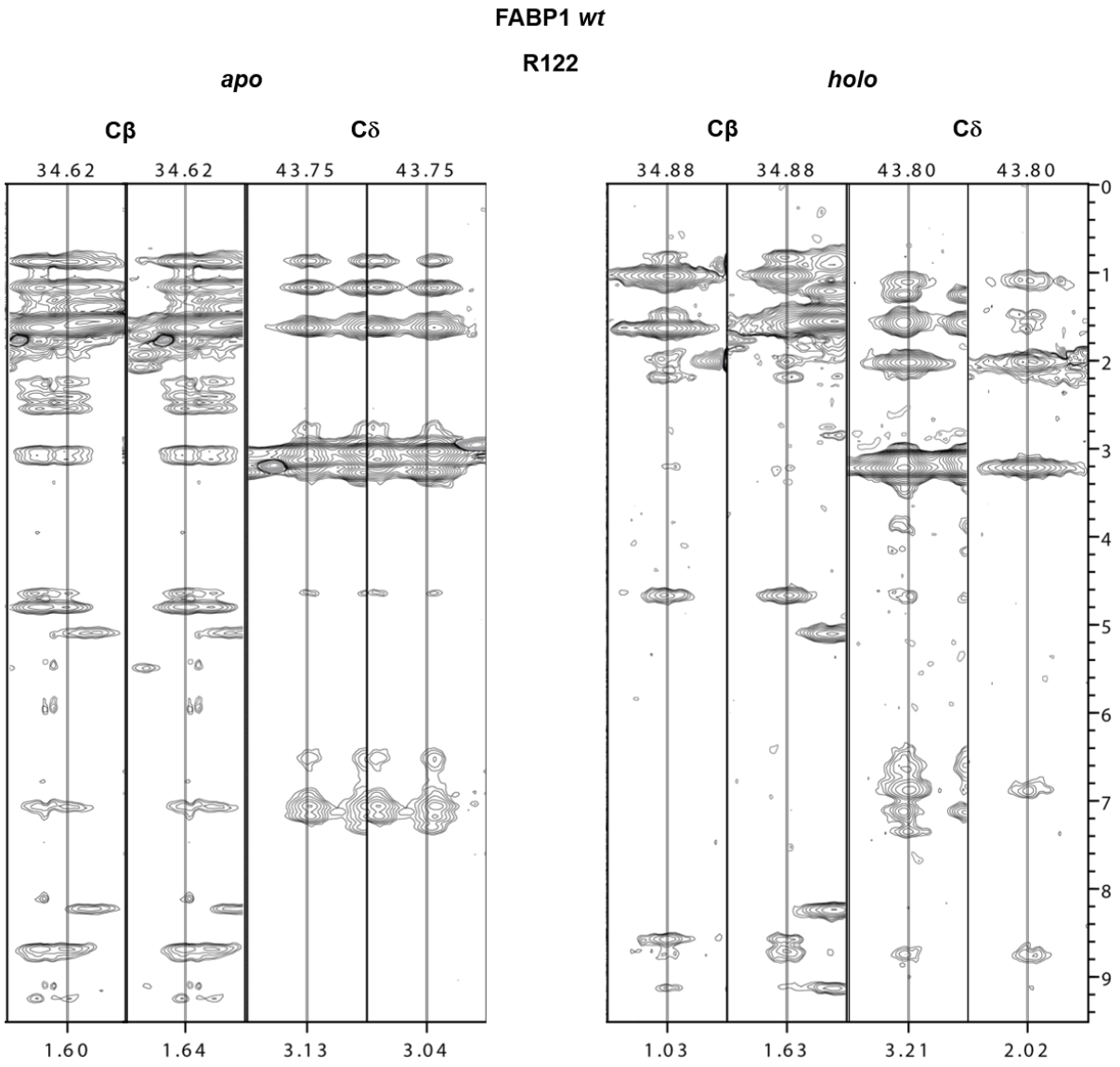

Supplementary Figure 11G. 2D [^{1}H,^{1}H] strips from 3D $^{13}C_{ali}$ resolved-[^{1}H,^{1}H]-NOESY spectrum of FABP1 in the absence (*apo*) and presence (*holo*) of GW7647.

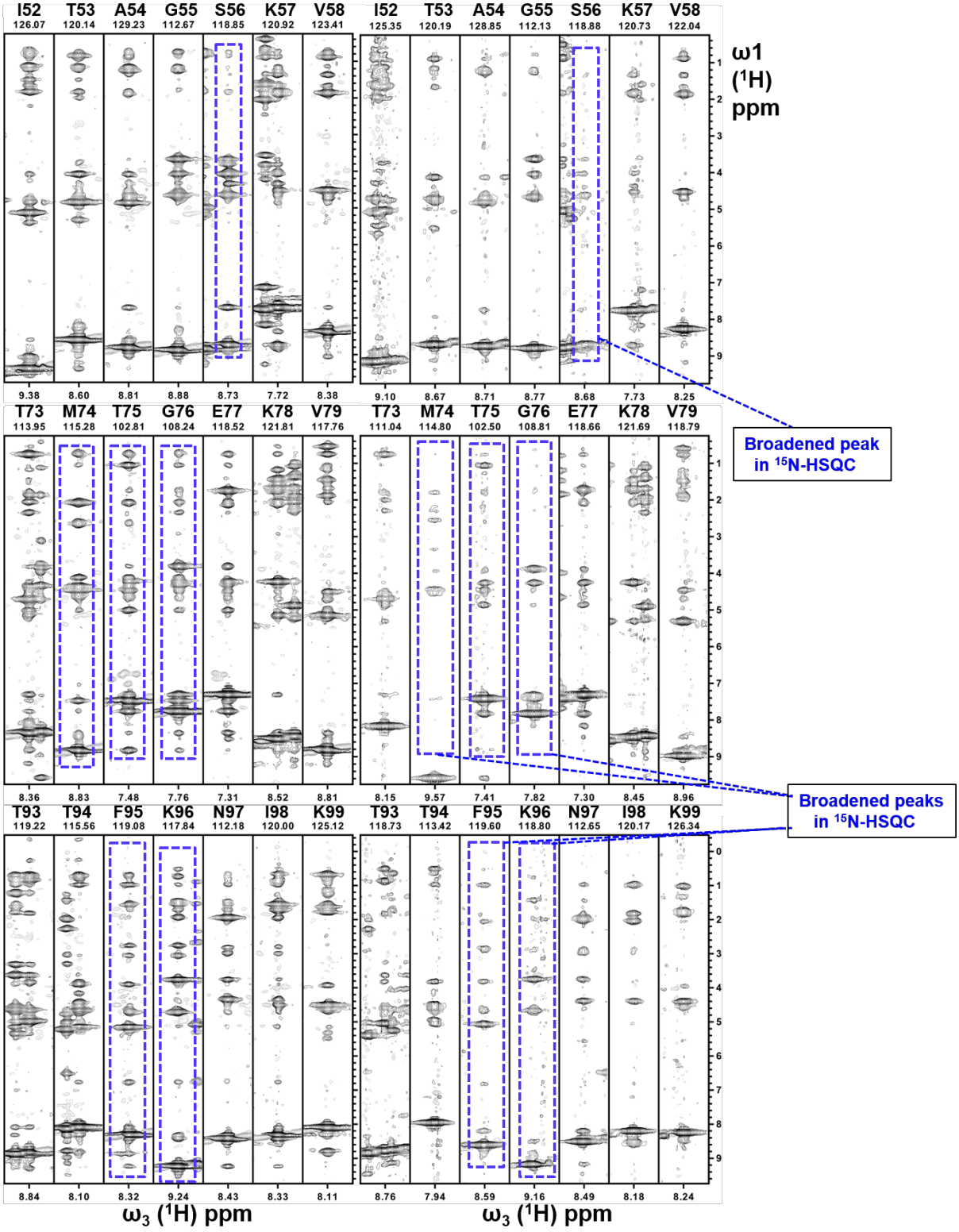

Supplementary Figure 12. 2D [^{1}H,^{1}H]-NOESY strips from 3D ^{15}N-resolved-[^{1}H, ^{1}H]-NOESY from [U-^{13}C,^{15}N]-labelled FABP1 in the absence (left) and presence (right) of GW7647. Several amide proton resonances are broadened in the presence of GW7647.

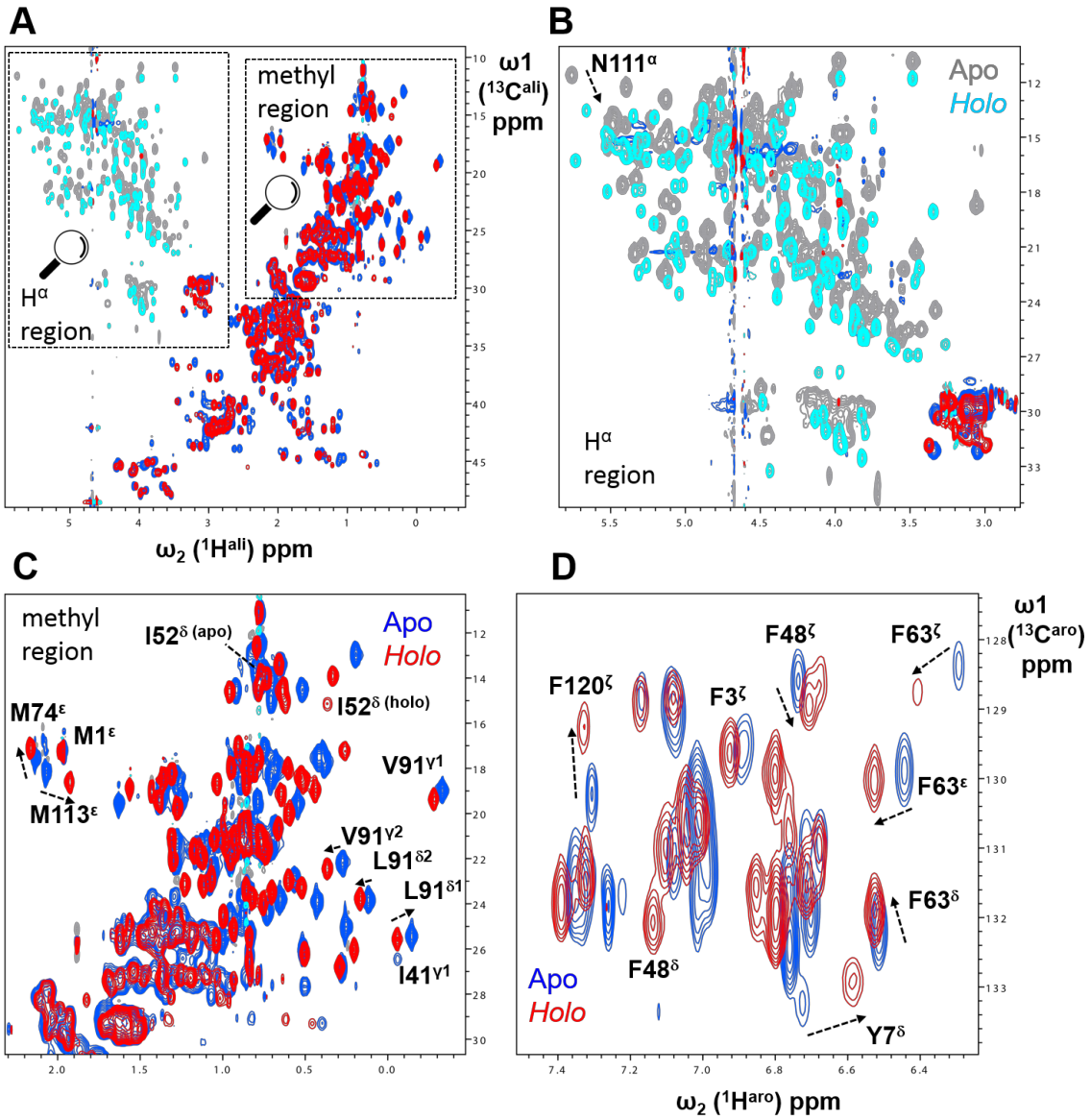

Supplementary Figure 13. (A-C) 2D [$^{13}C_{ali}$, ^{1}H]-HSQC **(D)** [$^{13}C_{aro}$,^{1}H]-HSQC of wt FABP1 in the absence (blue/grey) and presence (red/cyan) of GW7647.

Residues	atoms	Apo	Holo no GW7647	Holo with GW7647
all	all	0.69	0.82	0.77
all	backbone	0.32	0.49	0.43
all	sidechain	0.92	1.05	1.00
< 4A from GW7647	all	0.61	0.72	0.76
< 4A from GW7647	backbone	0.30	0.43	0.37
< 4A from GW7647	sidechain	0.79	0.91	1.00
> 4A from GW7647	all	0.71	0.85	0.78
> 4A from GW7647	backbone	0.33	0.51	0.44
> 4A from GW7647	sidechain	0.95	1.08	1.00

Table S1 Precision of FABP1 structures reported herein. RMSD of all atoms, backbone atoms only, and sidechain atoms only was calculated for different subsets of residues in 6DO6 (Apo); 6D07 (Holo no GW7647) and 6DRG (Holo with GW7647). Subsets consisted of all heavy atoms, atoms close to the ligand in the structures or atoms distant from the ligand in the structures. This analysis reveals that the apo structures have slightly higher precision than those of the holo protein, and there is little difference in the precision of residues close or distant from the ligand in either of the holo structures.

Residues	2l67(apo)	2l68 (Holo)
all	1.30	1.23
backbone	0.45	0.51
sidechain	2.07	1.89

Table S2 Precision of FABP1 structures reported 2L67 and 2L68. RMSD of all atoms, backbone atoms onlhy and sidechain atoms only for the structures of FABP1 calculated in the absence and presence of oleic acid.